water

MDPI

Article

Distribution and Demography of Antarctic Krill and Salps in the Atlantic Sector of the Southern Ocean during Austral Summer 2021–2022

Dmitrii G. Bitiutskii [1,2], Ernest Z. Samyshev [3], Natalia I. Minkina [3], Victor V. Melnikov [3,*], Elena S. Chudinovskih [3], Sergei I. Usachev [1], Pavel A. Salyuk [4], Alexander N. Serebrennikov [5], Oleg A. Zuev [6] and Alexei M. Orlov [6,7]

1 Sector of the World Ocean, Azov-Black Sea Branch of the Russian Federal Research Institute of Fisheries and Oceanography ("AzNIIRKH"), 344002 Rostov-on-Don, Russia
2 Environmental Biochemistry Laboratory, Institute of Biology of the Karelian Research Centre of the Russian Academy of Sciences (IB KarRC RAS), 185910 Petrozavodsk, Russia
3 A.O. Kovalevsky Institute of Biology of the Southern Seas of RAS, 299002 Sevastopol, Russia
4 V.I. Il'ichev Pacific Oceanological Institute Far Eastern Branch Russian Academy of Sciences, 690041 Vladivostok, Russia
5 Institute of Natural and Technical Systems, Russian Academy of Sciences, 299011 Sevastopol, Russia
6 Shirshov Institute of Oceanology, Russian Academy of Sciences, 117997 Moscow, Russia
7 Department of Ichthyology and Hydrobiology, Tomsk State University, 634050 Tomsk, Russia
* Correspondence: sevlin@rambler.ru; Tel.: +7-978-8292940

Abstract: The study aimed to investigate krill (*Euphausia superba*) and salp (*Salpa thompsoni*) populations in the Atlantic sector of the Southern Ocean in January and February 2022. Samples were obtained to measure the abundance, biomass and distribution patterns of krill and salp. Sex differences and feeding habits of the Antarctic krill were determined. The dependence of the physiological state of the studied aquatic organisms on changes in environmental parameters was analyzed. Current data on the association of the dynamics of hydrometeorological parameters and processes with the distribution of chlorophyll a, krill, and salp were obtained. It was established that, at numerous stations, the biomass of salps prevailed over krill. The result indicates the replacement of the Antarctic krill populations by gelatinous zooplankton. The obtained results allow assessment of the biological resource potential in the studied region based on the analysis of the samples collected.

Keywords: chlorophyll *a*; Euphausiacea; *Euphausia superba*; *Salpa thompsoni*; planktonic tunicate; climate change; feeding competition

check for updates

Citation: Bitiutskii, D.G.; Samyshev, E.Z.; Minkina, N.I.; Melnikov, V.V.; Chudinovskih, E.S.; Usachev, S.I.; Salyuk, P.A.; Serebrennikov, A.N.; Zuev, O.A.; Orlov, A.M. Distribution and Demography of Antarctic Krill and Salps in the Atlantic Sector of the Southern Ocean during Austral Summer 2021–2022. *Water* **2022**, *14*, 3812. https://doi.org/10.3390/w14233812

Academic Editor: Marina Marcella Manca

Received: 12 October 2022
Accepted: 17 November 2022
Published: 23 November 2022

Publisher's Note: MDPI stays neutral with regard to jurisdictional claims in published maps and institutional affiliations.

1. Introduction

The Antarctic krill *Euphausia superba* Dana, 1850 is one of the most abundant marine species of the Euphausiacea. It constitutes staple food for a wide range of animals and plays an important role in the functioning of Antarctic ecosystems and the Antarctic food web [1,2]. It has circumpolar distribution stretching from the coastal zone of the continental shelf to the northern boundary of the Antarctic Convergence. Due to its huge biomass and high biological value, it has become one of the important resources of the world's fisheries [3,4].

The maximum abundance of krill is observed in the Atlantic sector of the Southern Ocean (ASO), where its dense aggregations are formed in mesoscale gyres near seamounts and islands [5–7]. Over the past 80 years, krill abundance in the ASO has almost halved [8]. The extermination of whales in the 20th century did not lead to the expected increase in krill abundance: large baleen whales were replaced by penguins, fish, cephalopods, crabeater seals and small whales (Minke). The number of krill consumed by them exceeds the total diet of all baleen whales in the past by more than twice [9]. Current assessments

of the distribution and abundance of Antarctic krill in the ASO show that the prevailing environmental factors are primary production, population of predators (including the restoration of the population of whales and seals), surface water temperature, ice conditions, sharp climatic fluctuations, etc. At the same time, the impact of Antarctic krill fishing is considered to be minimal [10].

During summer, the adult part of the krill population is located in the surface water layer, usually above the seasonal pycnocline, at an average depth of about 50 m. They have an irregular spatial distribution, which can be explained by their active behavior. Krill often forms surface patches and can search for more favorable environmental conditions. Water dynamics can also have both a direct impact (cumulative effect of gyres) and an indirect one (for example, through changing of the phytoplankton abundance). The confluence of positive factors contributing to the formation of extensive and stable krill aggregations is most likely to happen in coastal/near-ice and near-island areas, where the topography slows down the system of gyres. In the oceanic zone, such aggregations are rare and exist for a short time until they disintegrate due to the frequent changes in hydrophysical conditions. Small aggregations of animals, represented by individual flocks, predominate here. The krill areas in the continental seas and adjacent waters are largely formed by the Coastal Antarctic Current and the circulation system by orographic and hydrological factors [11,12].

Despite the high fecundity of krill, its reproduction success depends on the possibilities of breeding in shallow waters, at the bottom of which krill eggs develop [12]. Several authors, using the 41-year-old (1976–2016) KRILLBASE-abundance [13] and KRILLBASE-length-frequency [14] databases, showed that the distributions of eggs, krill nauplii, and metanauplii had maximum intensity and success of spawning on the shelf and above the shelf slope. Association of the krill breeding zone with shallow waters clearly corresponds to the idea that the core of the population area is confined to the circulation of the Coastal Antarctic Current and the Weddell Sea.

Therefore, interannual fluctuations in the abundance of krill are mainly explained by its reproduction success (when spawning in shallow waters) and the intensity of the mechanical transfer of larvae and mature organisms away from spawning grounds by the currents during the intensification of meridional processes The latter also determines the abundance of other plankton (including phyto- and mesozooplankton) [12].

Krill abundance has been declining since the 1970s due to the penetration of salps into the high latitudes of the Southern Hemisphere [15–22]. Invasion of gelatinous planktonic animals, *Salpa thompsoni* Foxton, 1966, into the krill's core areas to the south of 60° S is followed by a dramatic increase in its abundance. The latter causes legitimate concern since the feeding rate of tunicates is high, and the diet composition of these species, i.e., salps, makes them feeding competitors of both krill and mesozooplankton [10,23]. Compared to other tunicates (ascidians, pyrosomes, doliolids), which draw food-containing water into the body using cilia, the salps have the functions of locomotion and food consumption combined. Salps swim and feed uninterruptedly pushing water through the esophagus with contractions of the muscles of the tunic and not experiencing saturation, which makes them a "biological pump". They have a "mucus" net that captures even tiny food particles which form food boluses with the help of slime [24]. This way of feeding makes the salp indiscriminate filter feeders. Salps are also well known for their fast growth rate among metazoans [25–27]. This way of feeding and a complex reproductive cycle also help salps increase their abundance [28]. Changes in the biomass and distribution of *S. thompsoni* are now considered a potential determinant of the future structure and functioning of the Antarctic and Southern Ocean ecosystems [29].

The purpose of our research was to obtain current data on the impact of changes in wind patterns, hydrological structure and water dynamics on the distribution of chlorophyll *a* fields and the abundance and biomass of krill and salps; we also aimed to assess the resource potential of the region based on biological data, including size, sex composition and examination of the physiological state of the animals.

2. Materials and Methods

Oceanographic studies were carried out in cruise 87 of the R/V Akademik Mstislav Keldysh in January–February 2022 [30] in the areas of the Bransfield Strait, Antarctic Sound, and the Powell Basin of the Weddell Sea, near the South Orkney, James Ross and Shishkov islands (latitude 65°–60° S, longitude 62°–41° W).

2.1. Remote Sensing Methods

Surface wind (SW) was studied using CCMP OCW vector data available with a 6-h temporal resolution and a spatial resolution of 0.25° × 0.25° [31]. Based on these data, averaged maps of the absolute dynamic topography (ADT) and absolute dynamic velocity (ADV) of the geostrophic current for the period from 15 January 2022 to 15 February 2022 were constructed. In the course of the work, daily maps of ocean surface temperature (OST) taken from the CMEMS with a spatial resolution of 0.05 × 0.05° [32] were also analyzed.

To analyze the spatial distribution of chlorophyll a, a map of satellite estimates of chlorophyll a concentration was drawn based on sea colour measurements from 15 January to 15 February 2022. To exclude omissions, use was made of the combined data of level 3 from satellite radiometers MODIS-Aqua, MODIS-Terra, and VIIRS-SNPP [33] with chlorophyll a concentrations from the chlor_a product, which uses the colour index algorithm (CI) [34] for low chlor_a values (<0.15 mg/m^3) and the OCx algorithm [35] for more productive waters. To build a map in each pixel of a regular 4-km grid, the median values of the chlorophyll a concentration between 15 January and 15 February 2022, were calculated.

2.2. CTD Measurements and Sampling

Hydrology. Our CTD data were obtained using an Idronaut OCEAN SEVEN 320Plus manufactured by Idronaut, Italy. The sounding complex was equipped with: a high-precision pressure sensor (PA-10X) with a measurement range of 0–100 Mpa, an accuracy of 0.01% and a resolution of 0.002%; two redundant temperature sensors with a measurement range from −5 °C to 45 °C, an accuracy of 0.001 °C, and a resolution of 0.0001 °C; two redundant conductivity sensors with a measurement range of 0–7 siemens/m, an accuracy of 0.0001 siemens/m, a resolution of 0.00001 siemens/m. The currents were measured using a TRDI Workhouse Monitor (Lowered Acoustic Doppler Current Profiler, LADCP) submersible acoustic Doppler profiler with a frequency of 300 kHz paired with a Shipborne Acoustic Doppler Current Profiler (LADCP) TRDI Ocean Surveyor-75 with a frequency of 75 kHz. Both profilers are manufactured by Teledyne Technologies Inc., 1049 Camino Dos Rios Thousand Oaks, CA 91360, USA. The obtained data were processed using the LDEO Software version IX.10 [36]. Additionally, tidal forces were taken into account and calculated using the software described in [37].

Chlorophyll a. Concentrations of chlorophyll *a* were measured on board by a standard spectrophotometric method based on the analysis of the absorption spectra of chlorophyll *a* extract in acetone [38]. Sea water was sampled at the stations by Niskin bathometers mounted on a rosette. Instrumental measurements of maximum chlorophyll *a* concentrations of about 6 mg/m^3 were performed on 28–29 January at 63.5–64.5° S, 55–56.5° W. Detailed information on the spatial distribution of the chlorophyll *a* concentrations was collected throughout the voyage by a continuous-flow laser fluorometer [39]; the intensity of chlorophyll *a* fluorescence was measured in motion with an interval of 60 s, which corresponded to approximately 300 m at a vessel speed of 10 knots. The seawater sampling depth was 5 m; the values of chlorophyll *a* fluorescence intensity were converted into chlorophyll *a* concentrations according to standard definitions data (38 points, R^2 = 0.9).

Macrozooplankton. Sampling was carried out in the late January and the first half of February 2022 in the western region of the ASO (Bransfield Strait (BS) and Antarctic Sound (AS), near the South Orkney Islands (SOI), the Powell Basin of the Weddell Sea (PB), near the islands of James Ross (JR) and Shishkov (SH) (Figure 1). The material was obtained from 34 hauls with the following fishing gear: double square net (DSN)—21 hauls, Isaak-Kidd

mid-water trawl modified by Samyshev-Aseev (IKMT-SA)—10 hauls and 3 catches with a standard Bongo net.

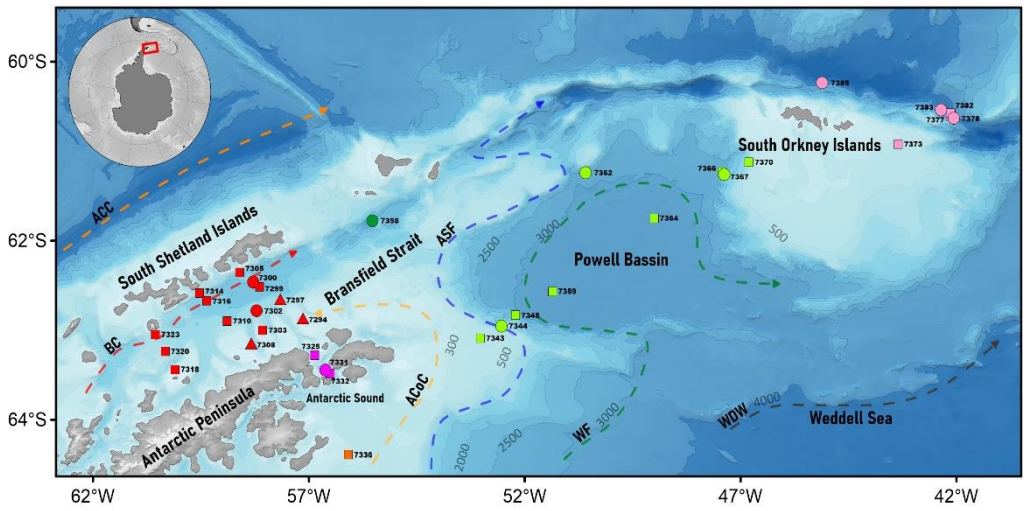

Figure 1. Map of the Antarctic krill and salp sample collection area with indication of currents (by: Heywood et al., 2004; Thompson et al., 2018). All stations were numerically marked. ACC—Antarctic Circumpolar Current, BC—Bransfield Current, ACoC—Antarctic Coastal Current, ASF—Antarctic Shelf Front, WF—Weddell Front, WDW—Weddell Deep Water. Fishing gear: ●—IKMT-SA, ■—DSN, ▲—Bongo net. Area: ●—BS, ●—AS, ●—PB, ●—SOI, ●—JR, ●—SH (designations according to Table 1).

Table 1. Number of krill and salp specimens studied by areas: Bransfield Strait (BS), Antarctic Sound (AS), South Orkney Islands Area (SOI), Powell Basin of the Weddell Sea (PB), James Ross Island area (JR), Shishkov Island area (SH).

Parameter	Number of individuals						
	BS	**AS**	**SOI**	**PB**	**JR**	**SH**	**Total**
Antarctic Krill							
Mass measurements	1140	548	733	743	500	125	3789
Biological analysis	734	330	529	543	300	125	2561
Salps							
Mass measurements	1549	-	2433	2136	-	303	6421

DSN—a double square net with an inlet area of 1 m^2 and a 6 m long filter cone made of gas with a mesh size of 0.5 mm [40], net was equipped with a water flow meter (Hydrobios, Germany) and a 24 kg wing-shaped depressor (Hydrobios, Germany). Oblique tows were carried out in layers starting from 730 to 100 m at vessel speeds from 2 to 3.1 knots. The towing depth was prompted by the pressure sensor readings of the Senti DT probe (Star Oddi, Iceland).

IKMT-SA—Isaacs-Kidd trawl modified by Samyshev-Aseev—is a non-closing trawl with a mouth area of 6 m^2, the net part is 25 m long and made out of a knotless net with a mesh of 6 mm and an insert at the trawl end of a nylon sieve № 15 (0.67 mm) [41]. Oblique tows were carried out in layers starting from 1900 to 440 m, at a vessel speed of 2.6–3.3 knots.

The Bongo net was a towed plankton net consisting of a frame with two metal rings, which had two filter cones with a mesh of 300 microns fixed on them. The diameter of each frame ring was 60 cm [42]. Oblique tow was carried out in layers starting from 270 to 130 m, at a vessel speed of 1.7–2.3 knots.

It should be noted that krill was obtained from catches using various types of gear (Bongo net, DSN, IKMT-SA) with fishing depths ranging from 100 to 1900 m. As Antarctic

krill can live at depths down to 800 m and the main concentrations of krill are in the depth range of 0–200 m, some measurements of the abundance and biomass of krill obtained from fishing with IKMT-SA at greater depths may be underestimates.

After trawling, each sample was weighed to an accuracy of 1 g and analyzed for composition. When the samples were large, the entire catch was weighed and a subsample (100–300 g) was taken out of it; the results of quantifying and weighing of such a subsample were extrapolated to the entire catch.

For biological analysis, a subsample of at least 300 specimens was taken. If there were fewer specimens in the catch, then it was analyzed in its entirety. For the calculation of biomass and abundance of Antarctic krill and salp aggregations, the data on each haul, tow depth and volume of filtered water per unit volume (1000 m^3) were taken into consideration [43]. Krill samples were processed following the generally accepted procedures and CCAMLR recommendations [44,45].

Biological analysis of freshly caught krill included measurements of the standard length from the outer edge of the eye to the end of the telson with an accuracy of 1 mm using a laminated paper scale [46]. Sex and maturity stage were determined under a UlabWF20X binocular (TM ULAB, China) with ×30 magnification or using a digital USB microscope ADSM 301 (Shenzhen Andonstar Technology Co., Ltd., Shenzhen, Guangdong, China) with digital zoom up to x4 according to the method of Makarov and Denys [47].

Stomach fullness (from 0 to 4 units, where 0 is empty, 4 is full), intestinal fullness (from 0 to 4 units, where 0 is empty, 4 is full), and liver colour were studied [48]. Each type of measurement was performed by the same person to minimize variability of results [49]. Krill specimens were weighed individually on a 20-g equal-arm mechanical scale VSM-20 (JSC Nizhny Tagil Medico-Instrumental Plant, Russia) with an accuracy of 10 mg (Table 1).

All sampled salps were fixed in 4–6% formalin for subsequent laboratory testing. Then a preliminary analysis of the selected samples was carried out by measuring the length of the salps with laminated graph paper by size groups with a step of 5 mm. Salps were weighed individually and in groups on a 20-g equal-arm mechanical scale VSM-20 (JSC Nizhny Tagil Medico-Instrumental Plant, Russia) with an accuracy of 10 mg (Table. 1).

3. Results

3.1. Hydrology

For the entire study area (latitude 66°–60° S, longitude 55°–40° W), we drew maps of ocean surface temperature (OST) with the surface wind (Figure 2) and absolute dynamic topography with geostrophic current velocities (Figure 3). In the tested area the heavy southeast wind (8 m/s) forked into the east and southwest winds (shown by arrows). The latter swirled in the cyclonic northwest direction (Figure 2). The swirling of the geostrophic current (shown by arrows) in the cyclonic direction was also observed (Figure 3). The wind and geostrophic vorticity led to a water rise in the cyclone centre with a simultaneous sea level lowering (the blue area in Figure 3). The lowering of the sea level occurred due to a higher density of deep waters compared to surface waters. The data in Figures 2 and 3 are averaged over the period from 15 January 2022 to 15 February 2022. Thus, the cyclonic vorticity, which led to the rise of deep waters during this period, was one of the reasons for the increased content of chlorophyll *a* (approximately at latitude 64° S and longitude 48° W).

CTD data for the upper 200 m layer show a spatial temperature distribution typical for the warm season (Figure 4). Positive temperature anomalies were recorded in the upper 50 m layer in most of the BS area and the coastal zones, while elsewhere a latitudinal dependence with a decrease in temperature values to the south was observed. At depths of 100–200 m, temperatures were below 0 °C, except for a narrow coastal strip along the South Shetland Islands associated with a current in the BS. Local temperature minimums were registered at the southernmost stations and on the southwestern slope of the Powell Basin.

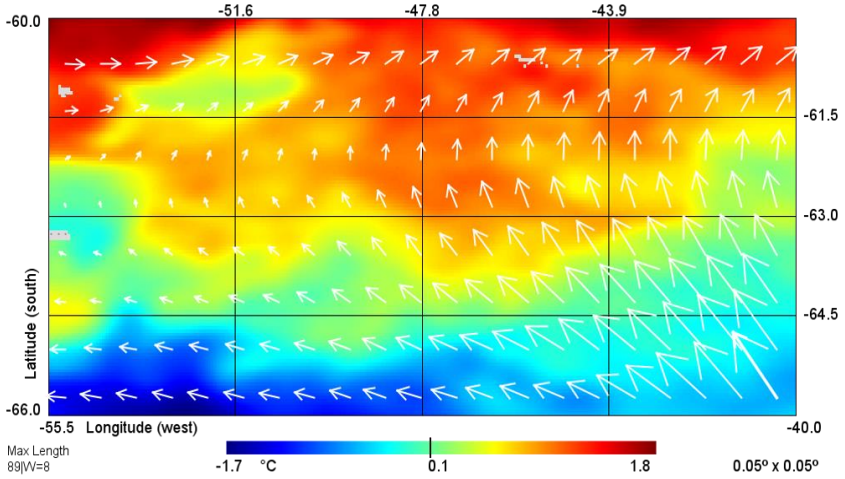

Figure 2. Spatial distribution of OST and SW (arrows) according to satellite measurement data (explanations in the text).

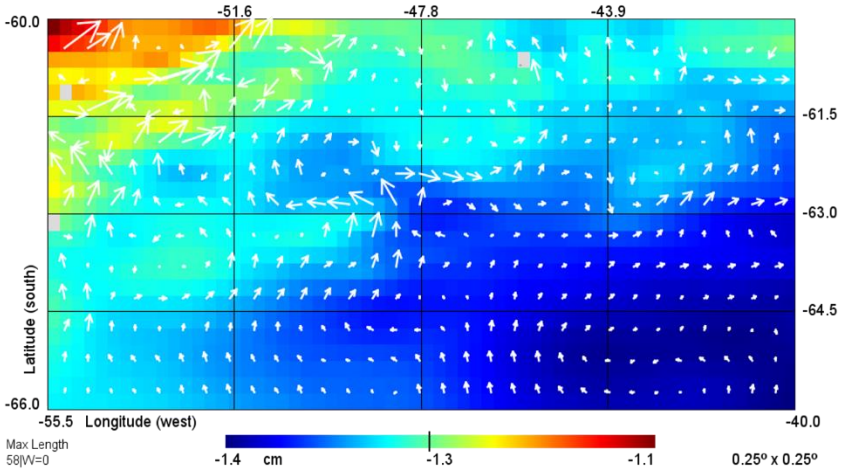

Figure 3. Spatial distribution of ADT and ADV (arrows) according to satellite measurement data (explanations in the text).

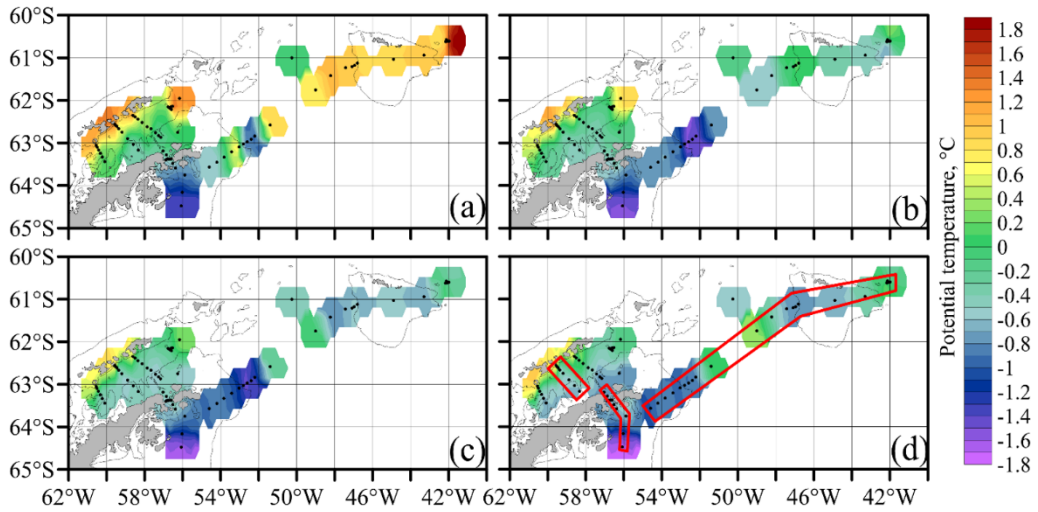

Figure 4. Spatial distribution of potential temperature on the horizons 50 (**a**), 100 (**b**), 150 (**c**) and 200 (**d**) m. The 500 m isobath is marked in grey. Stations are marked with black dots, sections are marked with red.

Most of the Bransfield Strait (Figure 5a,b) was occupied by the colder and saltier Transitional Zonal Water with Weddell Sea influence (TWW), which spread from north to south. Transitional Zonal Water with Bellingshausen Sea influence (TBW) and with the warm Bransfield current spread as a narrow jet close to the South Shetland Islands, reaching the middle of the strait only in the upper 50 m. The tentative boundary between these water masses runs along the 0 °C isotherms.

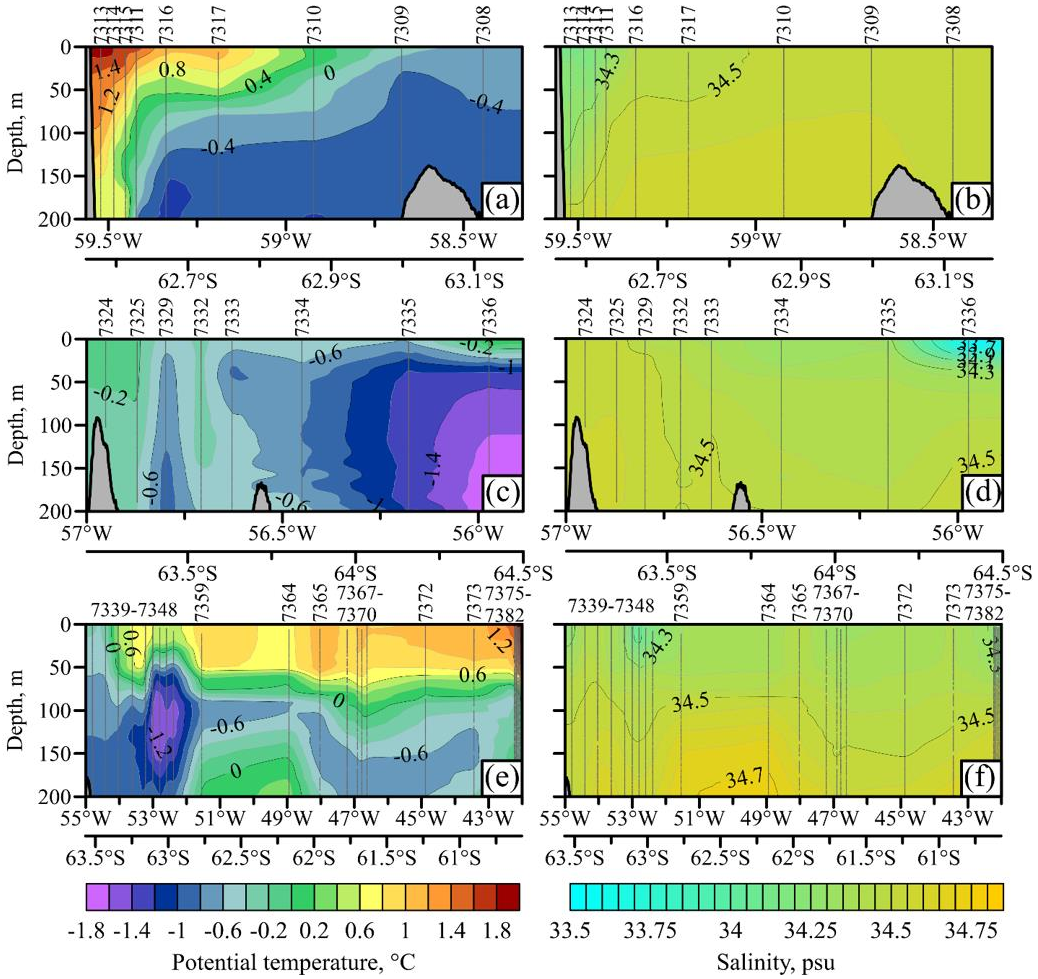

Figure 5. Potential temperature (**a**,**c**,**e**) and salinity (**b**,**d**,**f**) for three sections: the Bransfield Strait (**a**,**b**), the Antarctica Strait (**c**,**d**) and the Powell Basin (**e**,**f**). Station numbers are at the top, station positions are marked with grey lines. Seabed topography is shown on GEBCO2021 database. (https://www.gebco.net, accessed on 22 November 2022).

In the Antarctic Sound (Figure 5c,d), a decrease in temperature and salinity from north to south was observed. The northern shallow part of the strait was filled with the waters of the Bransfield Strait characterized by higher temperatures with a maximum of −0.10 °C in the upper 60 m layer and higher water salinity with a maximum of 34.55 parts per 1000 in the bottom layer. The deeper part of the strait was influenced by the waters from the Weddell Sea and by some freshening due to active ice melting.

The freshening was most pronounced in the upper 50 m layer (up to 34.29). Notably, st. 7336 to the south of the Antarctic Sound had outstanding minimum salinity values (33.55) and positive temperature values (0.10 °C) in the near-surface layer as well as greater gradients of thermohaline characteristics (at a depth of 200 m the values were −1.82 °C and 34.58).

The upper 200 m layer in the Powell Basin (Figure 5e,f) contained two water masses: the surface layer from 20 to 100 m in thickness was occupied by the Antarctic Surface

Water (AASW) formed during summer heating, while the underlying Cold Intermediate Water (CIL) between 50 and 150 m in thickness was the result of winter convection. In the AASW, the temperature increased from south to north from 0.50 °C to 2 °C; no latitudinal dependence was noted in the salinity distribution. In the CIL, the minimum temperatures were observed at the slope stations and reached −1.69 °C; the salinity increased smoothly with depth.

Strong near-surface currents observed in some subareas had a significant impact on the hydrological structure and water dynamics. The two-jet system of currents in the Bransfield Strait corresponded to the thermohaline structure: a powerful narrow jet to the northeast is the warm Bransfield Current (BC), while a weak wide jet to the southwest is a continuation of the Antarctic Coastal Current (ACoC). The highest ACoC velocities of 0.4 m/s were recorded on the shelf to the northeast of Joinville Island. A constant water flow from the Weddell Sea to the Bransfield Strait through the Antarctic Sound was not recorded; a cyclonic gyre was present in the southern part of the Strait.

3.2. Chlorophyll *a*

The highest chlorophyll *a* concentrations (more than 3 mg/m^3) were observed in the northern central and in the northwestern parts of the Weddell Sea (Figure 6). In the northern central part, increased values were recorded along the ice edge on 15–20 January; the chlorophyll *a* concentrations visible from the satellite gradually decreased to the values of about 1 mg/m^3 two weeks later. In the northwestern part of the Weddell Sea, on the shelf, high chlorophyll *a* concentrations were observed throughout the entire research period, both in the presence of an ice edge until 25 January, and later, until 15 February, when it was replaced by moving broken ice and icebergs.

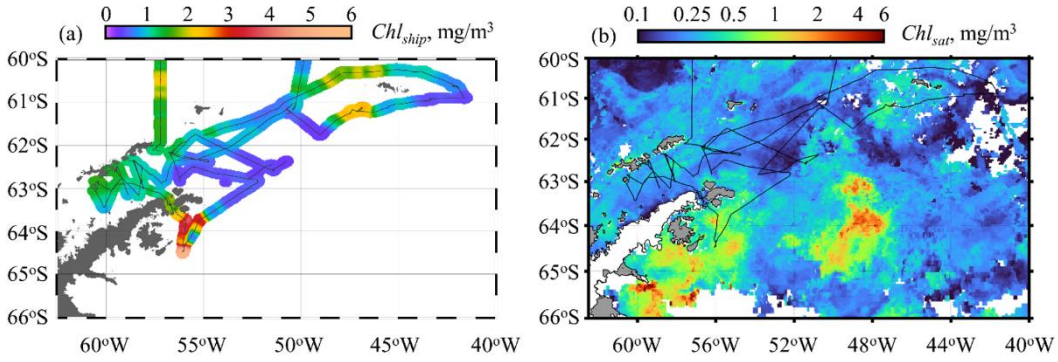

Figure 6. Spatial distribution of chlorophyll-a concentration (mg/m^3). (**a**) Flow-through fluorimetric measurements from 5 m depth while the vessel is under way; (**b**) median values of the combined satellite estimates from 15 January to 15 February 2022.

Average chlorophyll *a* concentrations (2–3 mg/m^3 according to ship data and about 1 mg/m^3 according to satellite data) were registered on the shelf of the South Orkney Islands in the direction of the southwest (7 February 2022) and northwest (12 February 2022). Relatively high values of chlorophyll *a* concentration (1–2 mg/m^3 according to ship measurements and 0.5–1 mg/m^3 according to satellite data) were observed in the Bransfield Strait closer to the South Shetland Islands.

The central part of the Powell Basin and the area to the east of the South Orkney Islands had very low chlorophyll *a* concentrations of less than 0.5 mg/m^3 and can, therefore, be classified as oligotrophic waters.

3.3. Macrozooplankton

Krill. The relative abundance of Antarctic krill varied from 0 to 537 individuals/1000 m^3. Its maximum values were recorded on the shelf to the north of the South Orkney Islands (Figure 1), where the IKMT-SA catch was ~33 kg. At this station, the trawling depth was

maximal −1900 m—while the acoustic equipment of the vessel registered krill accumulations at a depth of about 50–100 m.

To the southeast of James Ross Island a large spot of chlorophyll *a* was discovered, which was investigated with a DSN at a separate station. At a depth of 210 m, the relative abundance of krill represented by large immature individuals was 357 ind./1000 m^3. The third largest catch was in the Bransfield Strait with a relative krill abundance of 321 ind./1000 m^3. The main part of this catch consisted of juveniles. The relative biomass of Antarctic krill ranged from 0 to 331.8 g/1000 m^3. The two catches with the highest biomass were off the north of the South Orkney Islands and to the southeast of James Ross Island (331.8 and 207.5 g/1000 m^3, respectively), similarly to the catches with the highest abundance. The third largest biomass value was recorded in the Bransfield Strait (Figure 1)—73.4 g/1000 m^3.

Size and weight composition of krill catches Large-sized krill with a length of more than 45 mm prevailed near Shishkov Island, in the Antarctic Sound and in the area of the South Orkney Islands (50.7, 51.6, 80.8%, respectively). Medium-sized krill (35–45 mm) dominated the Powell Basin and off James Ross Island (51.3, 74.2%, respectively), and were also present in significant numbers in the South Orkney Islands area (48.6%). The minimum proportion of small-sized krill (<35 mm) was observed in the catches off the South Orkney Islands—0.7%, off the Shishkov Island—0.8%, in the Antarctic Sound—7.9%, in the Powell Basin—14.4%, off the James Ross Island—18.8%. In the Bransfield Strait, the proportion of small-sized krill was the highest and amounted to 80.7%. In the Bransfield Strait, 27 mm long krill prevailed among juveniles; adult lengths were 43 mm among females and 42 mm among males. In the Antarctic Sound, the individuals were 27, 46 and 50 mm long, respectively. In the area of James Ross Island, juveniles were dominated by 37 mm long individuals; such large juveniles were also found in the Powell Basin, in the Brasfield Strait, and near the South Orkney Islands. Both females and males in the area of James Ross Island were dominated by 40 mm long individuals. In the Powell Basin, 33 mm long krill typified the major part of the juveniles, adult females were mostly 45 mm long, and males were 40 mm long. In the waters near Shishkov Island, juveniles were represented by single specimens, whereas 48 mm long adult females and 47 mm long males predominated (Figure 7). The length-weight ratio of krill individuals was similar in all studied areas, all significant standard deviations being within the margin of error of individual measurements (Figure 8).

The results of cluster analysis allowed us to identify four krill groups according to their size composition (Figure 9). A violin-shaped graph was used to visualize the distribution of krill size data in various clusters. The main part of small-sized krill in cluster S was represented by juveniles 21–30 mm long; cluster M1 included medium-sized krill with body length of 35–41 mm, while medium-sized krill also prevailed in cluster M2, large individuals, 39–53 mm long, were also present in significant numbers; cluster L mainly included large-sized, 47–54 mm long, krill.

Small-sized krill (cluster S) were concentrated mainly in the Bransfield Strait near the shelf of the Antarctic Peninsula. Large krill (cluster L) were recorded in the deep part of the Bransfield Strait, in the area of Shishkov Island, in the northern part of the Powell Basin and the northeast of the South Shetland Islands. Large and medium-sized krill (cluster M2) were concentrated mainly in the Antarctic Sound, in the southwest of the Powell Basin and north of the South Orkney Islands. Medium-sized krill (cluster M1) were registered in the Antarctic Sound, in the southwest of the Powell Basin, south of James Ross Island, and in the Bransfield Strait.

Krill sex composition. The predominance of juveniles was noted only in the Bransfield Strait, whereas juveniles were also present in significant numbers in the catches off James Ross Island and in the Powell Basin (34.3%, 25.41%, respectively). Females largely predominated in the Powell Basin, where the female to male ratio was 2.6:1.0. Females also prevailed in the Antarctic Sound with a gender ratio of 1.3:1.0. The ratio of males and females near the South Orkney Islands was equal. Males prevailed slightly in the

waters near James Ross Island at 1.3:1.0 and to a large extent near Shishkov Island, at 4.1:1.0 (Figures 10 and 11).

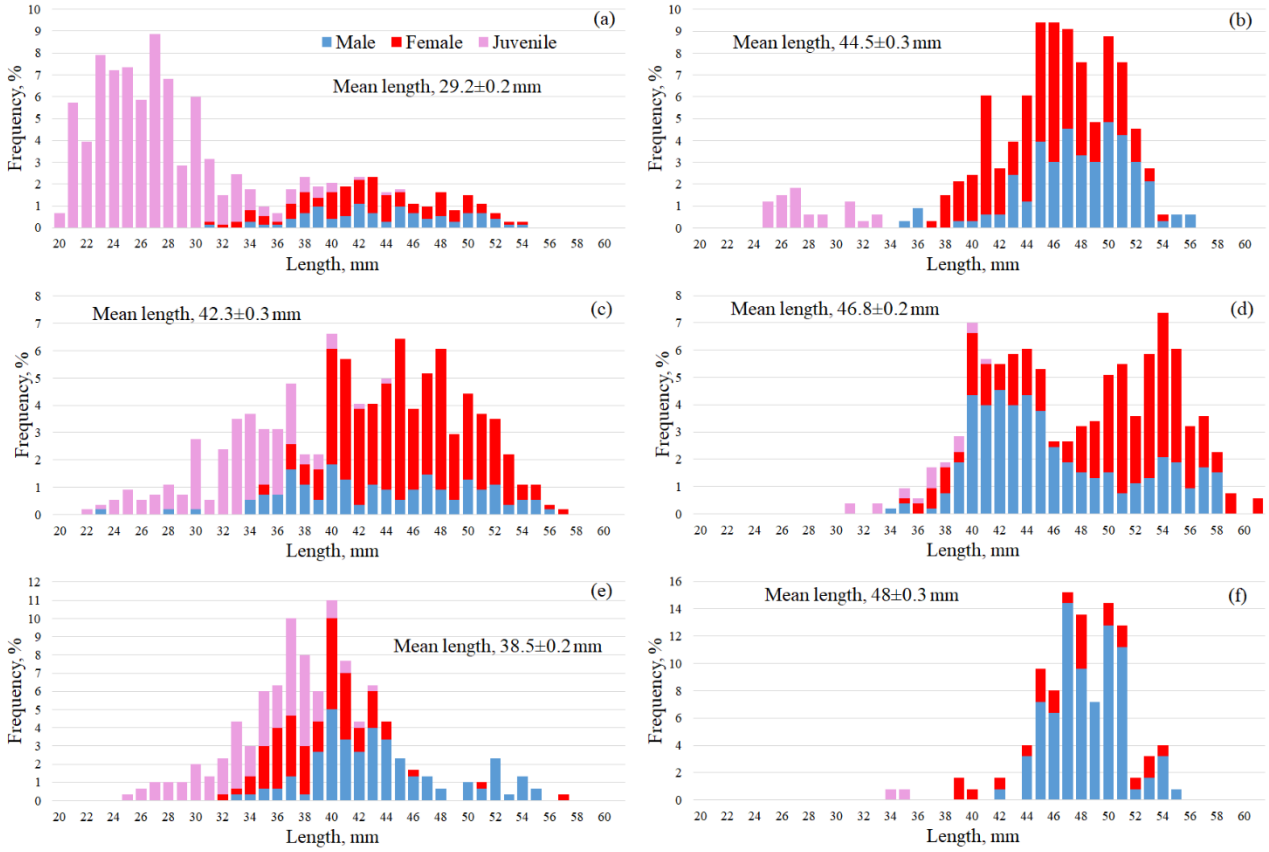

Figure 7. Size composition of Antarctic krill males, females, and juveniles in different areas: (**a**)—Bransfield Strait, (**b**)—Antarctic Sound, (**c**)—Powell Basin of the Weddell Sea, (**d**)—South Orkney Islands Area, (**e**)—James Ross Island area, (**f**)—Shishkov Island area.

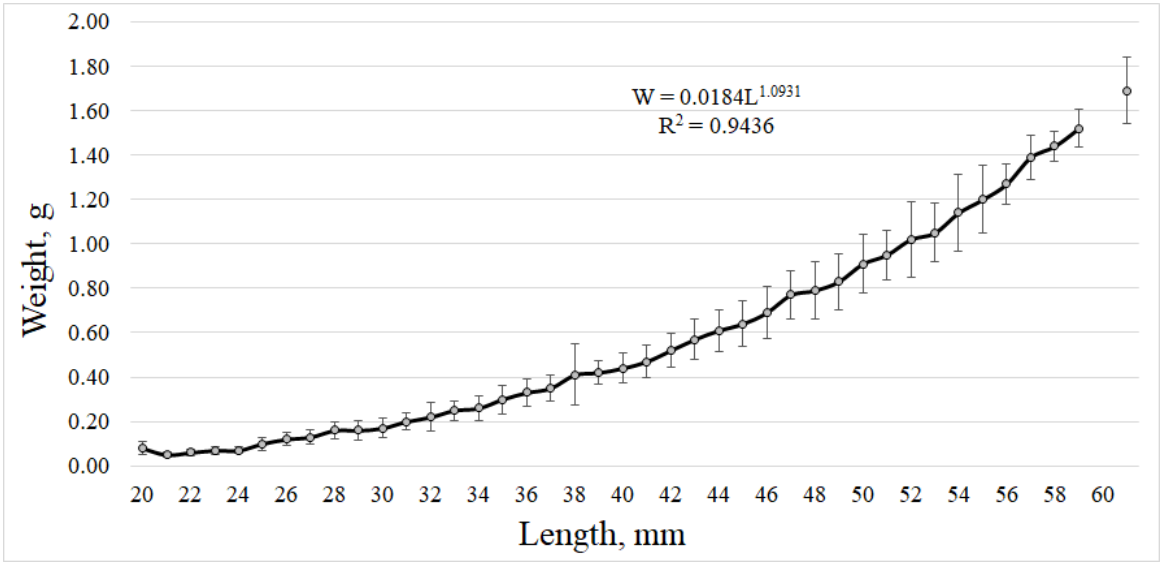

Figure 8. Relationship between the length and body weight of Antarctic krill in catches.

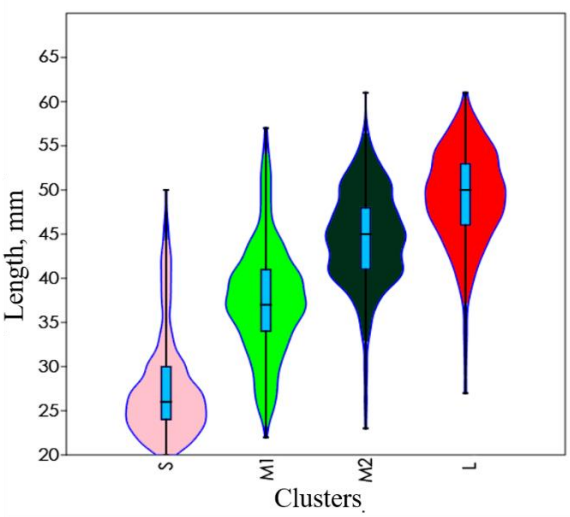

Figure 9. Krill distribution by size clusters ( )—interquartile range, —95% confidence intervals, |– median).

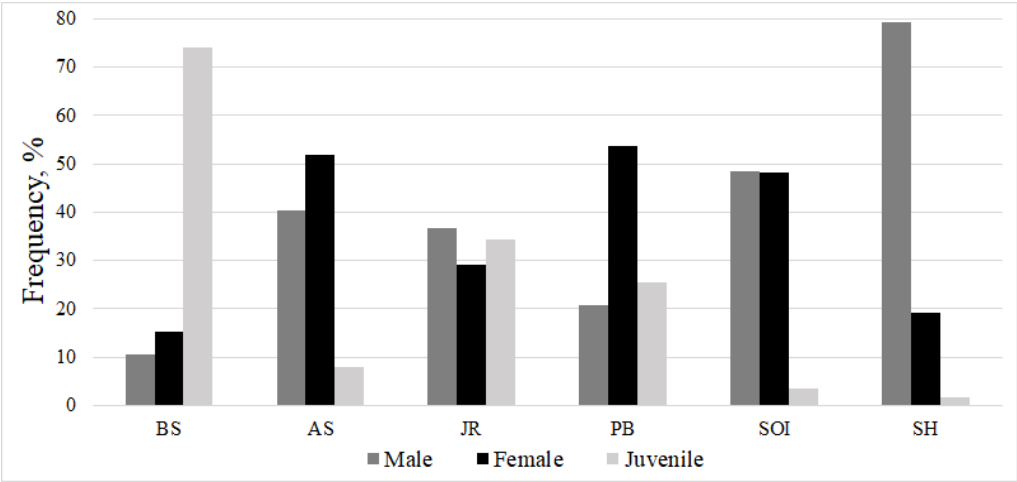

Figure 10. Ratio of Antarctic krill females, males, and juveniles in different areas (designations according to Table 1).

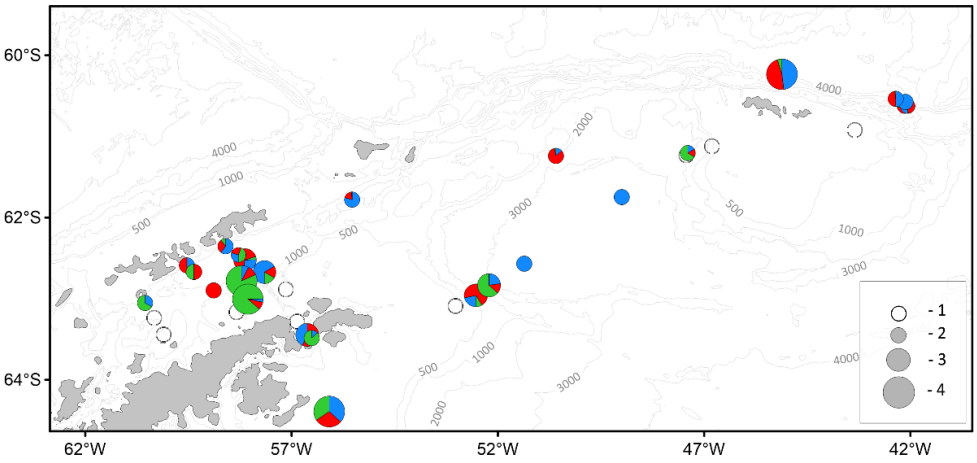

Figure 11. Spatial distribution of Antarctic krill relative abundance (ind./1000 m^3) and sex ratio (%) in ASO: —males, —females, —juveniles. Relative abundance (ind./1000 m^3): 1–0; 2–< 10; 3–11-100; 4–101-400.

Females which had completed spawning at the stage of maturity IIIE were absent in almost all catches; a small number of them (1.2%) were found near the South Orkney Islands, however. In this area, mostly females at stages IIIB and IIIC were registered—31.0% and 34.5%, respectively. In the Bransfield Strait, both mature pre-spawning females at stage IIIB (35.5%) and immature females with a fully formed thelyum at stage IIB (34.6%) prevailed.

In the Antarctic Sound, females at stages IIIB and IIIC predominated, at 39.8% and 41.0% of the total, respectively. In the Powell Basin and near Shishkov Island, females at stage IIIB also largely dominated, as 54.8 and 58.3%, respectively. In the James Ross Island area, 74.7% of females were at stage IIB (Figure 12).

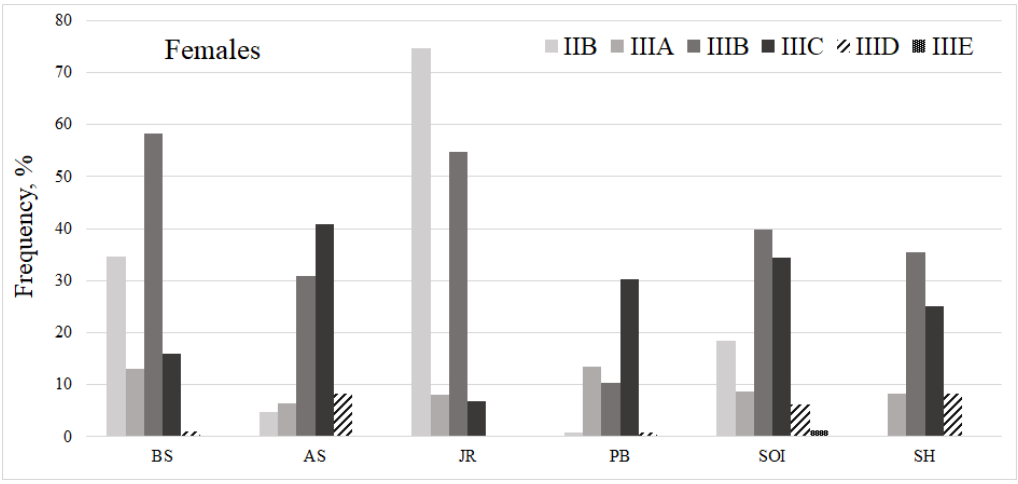

Figure 12. Proportion of Antarctic krill females at different stages of maturity (%) by area (designations according to Table 1).

Females at stage IIIA were present in all areas (6.0–13.5%). Females at stage IIID were present in all areas but in small numbers (1.0–8.3%), except for the area near James Ross Island, where females at this stage of maturity were absent.

Generally, the largest number of females was represented by pre-spawning individuals at stages IIIB (39.1%) and IIIC (29.4%) in the study areas. Females at the last stage of maturity IIID as well as females that had spawned were almost absent in the catches and accounted for 3.8% and 0.3%, respectively. Females at early stages of maturity (IIB and IIIA) were present in small numbers (17.2% and 10.2%, respectively). The majority of males in the Bransfield Strait (99.2%), near James Ross Island (96.4%), in the Powell Basin (68.8%), and near the South Orkney Islands (73.8%) comprised individuals at stage IIA (Figure 13).

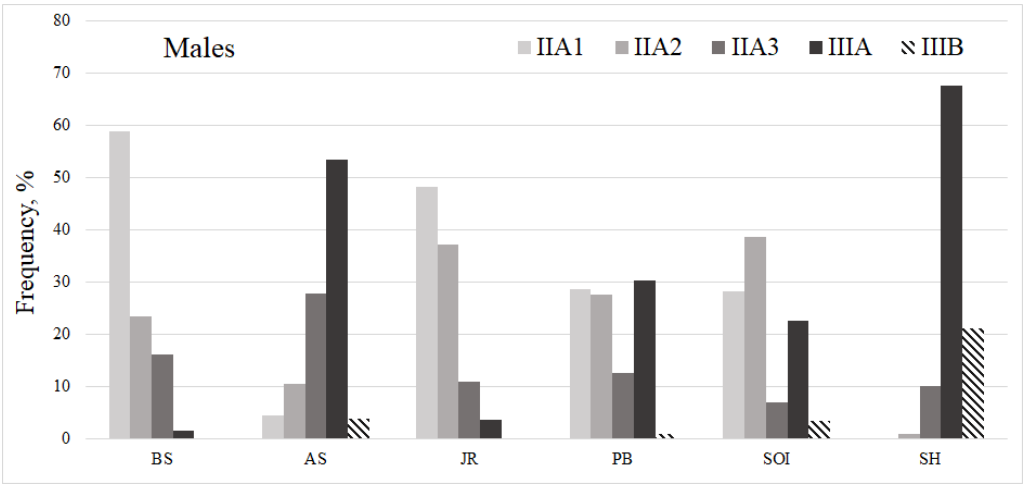

Figure 13. Proportion of Antarctic krill males at different stages of maturity (%) by area (designations according to Table 1).

Mature males prevailed in the Antarctic Sound and near Shishkov Island (IIIA accounted for 53.4% and 67.7%, respectively, and IIIB—3.8% and 21.2%, respectively). In the Powell Basin, the proportion of mature males was 30.4% (IIIA) and 0.9% (IIIB), while in the area of the South Orkney Islands, they accounted for 22.7% (IIIA) and 3.5% (IIIB).

The maturation ogives of male and female Antarctic krill from late January to mid-February are shown in Figure 14. Mass maturation (body length at 50% sexual maturity) $L_{50\%}$ occurs in 45 mm Antarctic krill for both males and females.

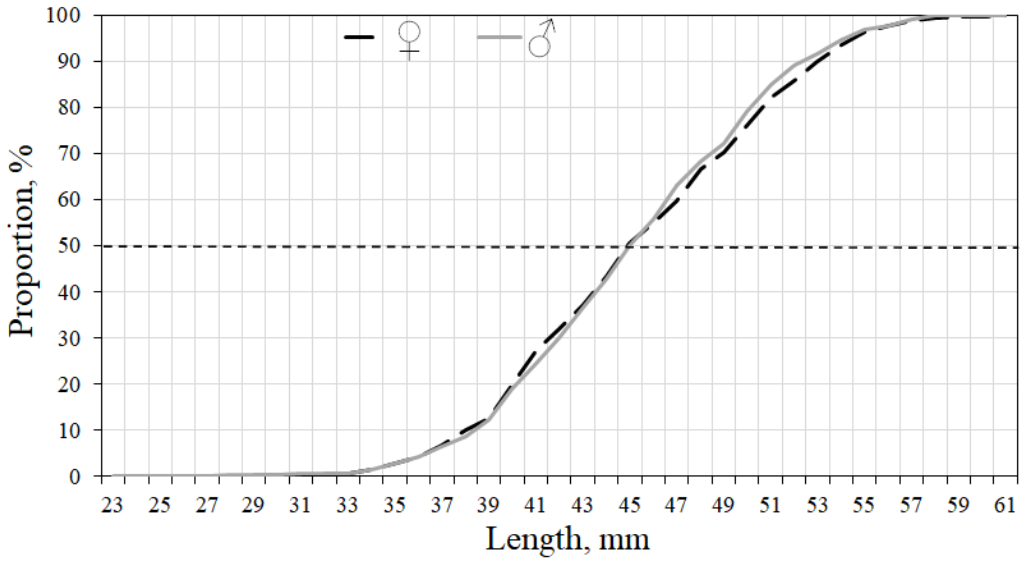

Figure 14. Maturation ogives of males (♂) and females (♀) of Antarctic krill in ASO.

Krill feeding. During the study period, krill actively fed in all areas, as evidenced by the data on the average value of stomach/intestines fullness of mature and juvenile individuals (Table 2). The stomach/intestines fullness of the juveniles was, on average, lower than that of mature males and females. The krill actively fed in the Bransfield Strait (3.7/1.9 units), in the Antarctic Sound (3.9/2.1), near the South Orkney Islands (3.3/1.4), in the area of James Ross Island (3.6/2.0) and Shishkov Island (3.7/1.3 units). The lowest feeding intensity, 1.7/0.7 units, was observed in the Powell Basin.

Table 2. Filling of the stomach/intestines (average score) of Antarctic krill in various research areas (designation of areas according to Table 1).

	BS	AS	SOI	PB	JR	SH	Average Score
Juvenile	3.6/1.8	3.4/2.2	2.5/0.5	0.5/0.2	3.4/1.7	1.0/0.0	2.7/1.3
Females	3.8/1.7	4.0/2.3	3.6/1.6	2.8/0.9	3.4/2.4	3.4/0.6	3.5/1.5
Males	3.9/2.3	3.9/2.1	3.0/1.2	1.9/0.9	3.8/2.3	3.8/1.5	3.3/1.6

Due to active feeding, almost all krill had light-green or dark-green livers (Figure 15). Krill with transparent liver was present in all study areas but accounted for only 0.3–5.0%. Krill with a yellowish liver was caught in the Powell Basin—11.7%, off the South Orkney Islands—7.3%, and also near Shishkov Island—3.4%.

Salps. The relative abundance of salps varied from 0 to 202 ind./1000 m^3. The largest concentration of salps, 201.5 ind./1000 m^3, was found in the central part of the Powell Basin in the Weddell Sea. The highest concentrations of salps were all across the section through the Powell Basin, to the east of the South Orkney Islands, in the northern and western parts of the Bransfield Strait. Krill dominated to the north of the South Orkney Islands, in the shelf zone of the southwestern part of the Powell Basin, and the south of the Bransfield Strait in the Antarctic shelf zone. The krill only areas were found in the Antarctic Sound

and the southeast area of James Ross Island. Salps were also present at a ratio of 4:1 near Shishkov Island.

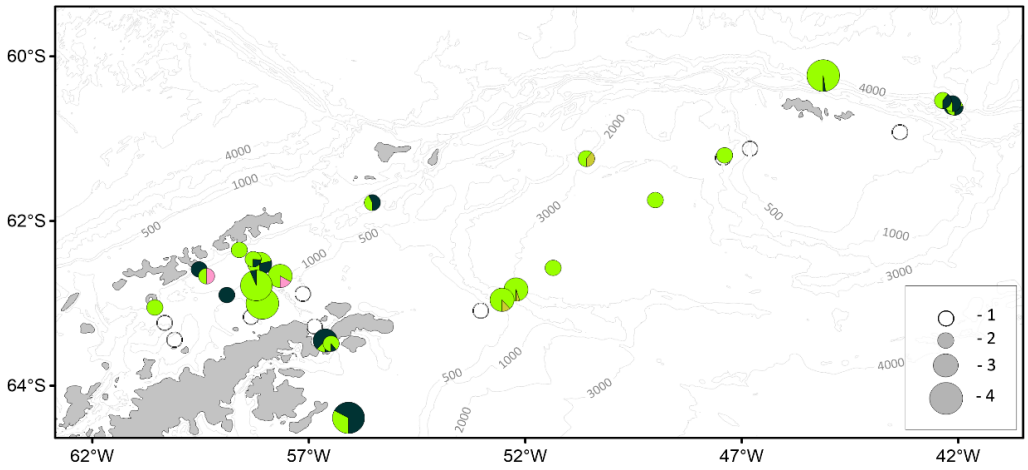

Figure 15. Distribution of Antarctic krill in study area by liver color: ●—light-green, ●—dark-green, ●—yellow, ●—milky white. Relative abundance (ind./1000 m^3): 1–0; 2–< 10; 3–11-100; 4–101-400.

The relative salp biomass varied from 0 to 72 g/1000 m^3 with its maximum value recorded in the Bransfield Strait (Figure 16). The distribution of the relative abundance and biomass of krill and salps had similar patterns.

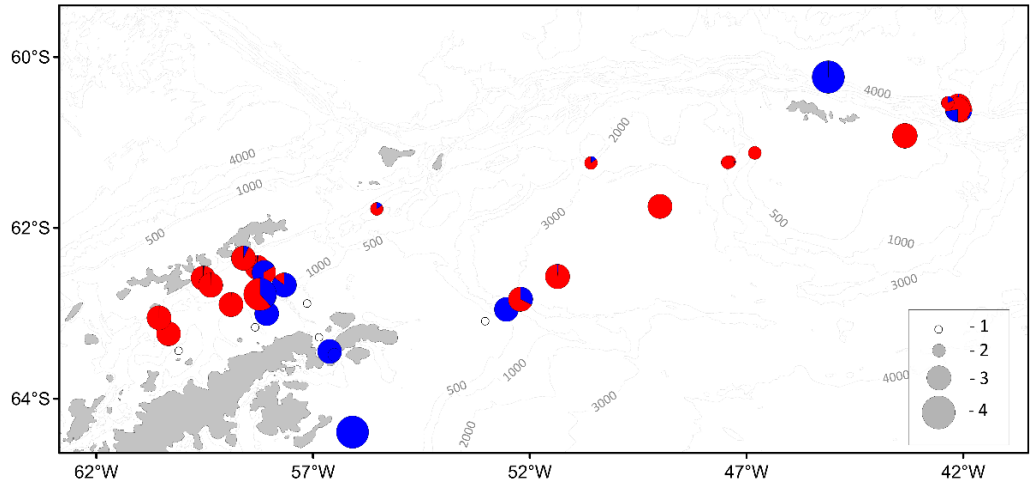

Figure 16. Spatial distribution of relative biomass (g/1000 m^3) and proportion (%) of Antarctic krill (●) and salps (●). Relative biomass (g/1000 m^3): 1–0; 2–< 10; 3–11-100; 4–101-350.

The only difference was the presence of large aggregations of small-sized krill and medium-sized salps in the shelf zone of the Antarctic Peninsula in the south of the Bransfield Strait (Figure 17), which resulted in a lower number of salps but their larger biomass.

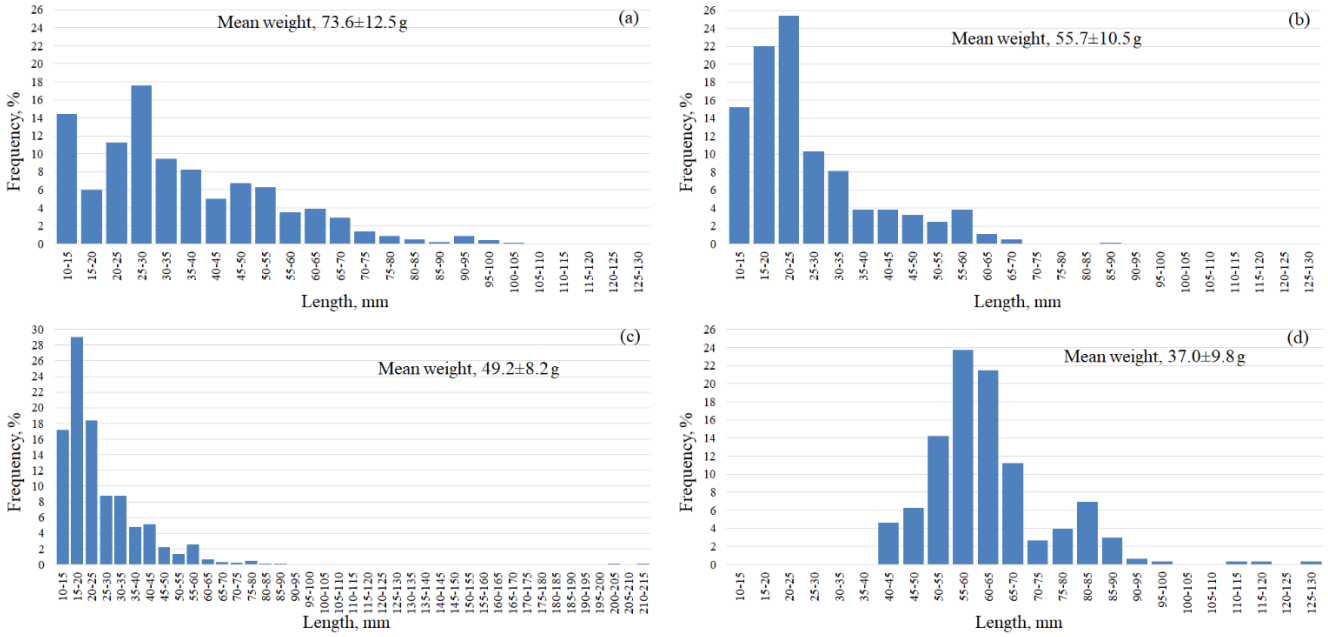

Figure 17. Size composition of salt Salpa thompsoni in different areas: (**a**)—Bransfield Strait, (**b**)—Powell Basin of the Weddell Sea, (**c**)—South Orkney Islands Area, (**d**)—Shishkov Island area.

4. Discussion

The results of our studies showed that the thermohaline structure and dynamics of the waters were in good agreement with established ideas about the hydrophysical processes in this zone [50–52] and corresponded to the data of recent years [53–55]; however, significant local differences were also observed. Thus, in the Bransfield Strait, a greater southward spread of TWW along the entire strait was recorded compared to the data of 2013 [56]; the waters of the Antarctic Sound were significantly warmer compared to the same period in 2020 [57]. There was no constant inflow of water from the Weddell Sea to the Bransfield Strait through the Antarctic Sound, the structure of the currents was variable, which was also confirmed by the recent studies in this area [58].

The spatial distribution and concentrations of chlorophyll *a* also corresponded to the results of the previous studies. In January 1995, at the ice edge in the northwestern and central parts of the Weddell Sea, chlorophyll *a* concentrations exceeded 5 mg/m^3 and reached 13 mg/m^3 [59]. In February 2015, low concentrations of chlorophyll *a*, 0.32 $\pm$ 0.02 mg/m^3, were recorded in the southeast of the South Orkney Islands and average concentrations of 1.87 $\pm$ 0.22 mg/m^3 to the north and northwest of the South Orkney Islands [60]. Obtained data most resembled the results of February–March 2008 and 2009 [61] which were as follows: concentrations of less than 0.5 mg/m^3 occurred in the central part of the Weddell Sea (AASW waters) and the zone of influence of the Weddell Sea in the Bransfield Strait (TWW waters); 0.5–1.5 mg/m^3—in the Bransfield Strait closer to the shelf of the South Shetland Islands (TBW waters); more than 2 mg/m^3 with peaks up to 4–7 mg/m^3 to the east of James Ross Island in the northwestern area of the Weddell Sea near active ice melt. Satellite estimates of the chlorophyll *a* concentration in the Antarctic Peninsula area were lower than the contact ones, which is associated with the regional optical characteristics [62,63]. Therefore, satellite maps of the chlorophyll *a* concentration should be analyzed for structural features of the pigment distribution, not the values per se. The general patterns of the spatial distribution according to the data of satellite and contact measurements of the chlorophyll *a* concentration were similar. Satellite data provide more information on the areas adjacent to the expedition route, and the ship measurements provide more accurate data for certain points of the route. Thus, in the central region of the Weddell Sea, according to our contact measurements, no high concentrations of chlorophyll *a* were recorded.

However, the satellite map showed that there were zones with increased concentrations of chlorophyll *a* nearby, most probably due to the abundance of phytoplankton near the ice edge, which corresponds well with the results of the previous studies in the northwestern Weddell Sea [59].

Hydrological data and satellite observations for our study period indicated the transfer of Antarctic krill from the Weddell Sea to the Bransfield Strait with a cold ACoC current carrying colder and saltier TWW waters from the Weddell Sea. The maximum abundance of Antarctic krill in the Bransfield Strait (the shelf of the Antarctic Peninsula), as well as in the Antarctic Sound, was associated with a combination of favourable environmental factors (temperature, salinity, and abundance of phytoplankton). In the Bransfield Strait, such conditions were formed under the influence of the TWW with the temperatures of −0.8 to 1.7 °C, which were optimal for the growth and development of both juveniles and mature krill individuals [64–66]. In the Antarctic Sound, the main biomass of Antarctic krill was also formed by krill brought from the Weddell Sea. The obtained data are consistent with the view that immature individuals tend to colder waters, unlike mature individuals [13,67]. Salinity variability seemed not to significantly affect the distribution of krill at different stages of development, for which the range of 34.5–34.6 is optimal. The maximum abundance of krill was noted around station 7336 (Figure 1), which was characterized by the minimum salinity (33.55) in the surface layer, positive values of potential temperature (0.1 °C), and high chlorophyll a concentration (>20 mg/m^3), whereas, at a depth of 200 m, the potential temperature was close to the freezing point of seawater (−1.8 °C), salinity was higher, and the concentration of chlorophyll a did not exceed 0.5 mg/m^3.

In the ASO, the average abundance and biomass of krill correlated well with the data obtained in 2019–2020. However, our results for the density of Antarctic krill aggregations in the Antarctic Sound were almost ten times higher than before [68,69]. Large accumulations of salps were registered in the Bransfield Strait, which is associated both with the influence of the warm BC current [70] and with the peculiarities of feeding and reproductive cycle of salps [28]. The findings on the presence of large aggregations of Antarctic krill in the Antarctic shelf of the Bransfield Strait are consistent with the previous studies [43,71].

The size composition of Antarctic krill varies greatly from year to year in the same study area. According to our results, small-sized krill (82%) prevailed in the Bransfield Strait, whereas, in the same ASO area, only 22% of small-sized krill were found by the 2020–21 expedition [72] and only about 40% by the 2019–20 expedition [68]. A similar situation was observed in other regions. The reasons for such discrepancies could be natural fluctuations in the size structure or differences in research methods, which therefore require standardization. In particular, a repeated grid of stations is required for correct comparisons of the obtained results and the use of large fishing gear similar in design and size since krill can slip away out of small samplers [73,74]. Moreover, the entire layer (0~200 m) of the Antarctic krill habitat needs to be sampled [75,76]. However, despite all of the above, the feeding characteristics of krill remain the main factors determiningits size compositions [6,7]. In some study areas, the catches included large individuals of krill (up to 45 mm) without clearly expressed sexually dimorphic features (insufficiently developed petasma and almost undeveloped internal genitals). The explanation of this phenomenon could be found, with high probability, in the feeding conditions of krill [77–79], which is also evidenced by the fatty acid analysis of its individuals [80]. It can be assumed that under these conditions the growth of krill individuals is ahead of their development.

The sex composition of krill differed significantly from one of the previous years. So, in the area of the Bransfield Strait and Antarctic Sound and eastward of the Antarctic Peninsula (the Weddell Sea) the number of juveniles of different sizes was significantly higher than in other researched areas, which was not observed in the recent studies [68,69,71,72]. At the same time, in January–February 2020, a significant number of spent females were found in almost all the studied areas [72], while in our study, spent females were found near the South Orkney Islands only. In ASO, the number of juveniles caught did not exceed 33%,

while in the recent study this value did not exceed 10% [72]. The maturation ogives of male and female Antarctic krill indicate the same development of both genders up to the length of sexual maturity $L_{50\%}$, after which females grow more slowly than males. This pattern was also noted previously [77]. The condition of sexual maturity of krill impacts greatly on this relationship.

Antarctic krill is an active filter-feeder and feeds mainly on phytoplankton [79,81]. As was shown earlier, the decrease in the active feeding of krill occurs mainly in the autumn and winter periods, while the feeding activity increases towards the end of spring [48]. Our data also testify to the active feeding of krill in the austral summer period.

We recorded an almost complete absence of krill at the stations in the Powell Basin. This area was studied by various expeditions on different sections [68,69,71,72,82–85]. Overall, the compilation of data for research regions shows much similarity. Thus, in the Powell Basin, as well as in the waters near the South Orkney Islands, water temperature regime (with the warming up to 2 °C) is favorable for the development of salps. Earlier publications reported active salp development after winters with relatively low sea ice development [6,7]. Unlike krill, the salp propagation does not depend on the ice cover and the associated algae, which are the main prey for krill larvae and juveniles [86]. At the same time, the life cycle of salps is much shorter than that of krill, and the fluctuations in their abundance reflect the annual variability of conditions contributing to massive population growth [87–89].

5. Conclusions

The analysis of the obtained data demonstrated significant shifts in the thermohaline structure and currents of the upper 200-m water layer in the Antarctic Peninsula area. A stronger southward spread of TWW was noted along the entire Bransfield Strait. The upper layer of the Antarctic Sound waters became significantly warmer, and an extremely small amount of ice was observed. The maximum values of chlorophyll *a* concentration of more than 5 mg/m^3 were observed only on the shelf in the northwestern Weddell Sea, where the transport of icebergs and broken ice was registered. Waters with the lowest concentrations of chlorophyll a (less than 0.3 mg/m^3) were found in the central part of the Powell Basin, in the area to the east of the South Orkney Islands, and in the Bransfield Strait near the Antarctic Peninsula. Judging by the chlorophyll a concentration values, both oligotrophic and mesotrophic waters are present in the study area. Mesotrophic waters, with chlorophyll a concentrations of more than 2 mg/m^3, were observed mainly in the shelf areas in the northwestern part of the Weddell Sea and to the west of the South Orkney Islands, as well as in separate zones at the edge of ice fields in the Weddell Sea.

This results also demonstrate a close relationship between Antarctic krill and salps and a combination of such environmental factors as surface water temperature and availability of forage. The circulation of water masses within the region play into the dynamics of this interaction. Only in the Bransfield Strait and to the south of the Antarctic Sound at the boundary of packed ice, in the relatively warm and desalinated surface layer and in combination with the cold and salty subsurface water layer, were the optimal conditions for the maximum concentrations of Antarctic krill formed. The reasons for the relatively low krill reproduction in the study area may be found in the late spawning period and, consequently, the low survival rate of krill larvae. The data on Antarctic krill abundance for the latest decade have shown significant fluctuations in the ASO [8,10,15,90,91].

Thus, our results indicate the need to continue long-term monitoring of this area, where the euphausiid biomass has traditionally been one of the largest in the entire Antarctic [12]. Climate changes gradually lead to significant seasonal and interannual fluctuations in the abundance of these crustaceans against the background of an ever-increasing abundance of salps [8,14,15]. Differences in the abundance of salps and krill can be explained by differences in the ice cover in the ASO in other years, the extent of which determines the availability of food for these planktonic animals: at high ice coverage, salps are limited in food, while krill are able to "gnaw it out of the ice" [15,92]. The result indicates the

replacement of the Antarctic krill populations by gelatinous zooplankton a steady long-term tendency towards a decrease in the population of Antarctic krill (from 38% to 75% per decade) and its successive replacement by salps in this water area [8,14,15,90]. Such changes may affect the structure and productivity of the Antarctic ecosystem as a whole [8,10,91,93].

Author Contributions: Conceptualization by E.Z.S. and A.M.O.; methodology and validation by D.G.B. and N.I.M.; formal analysis and original draft preparation by V.V.M. and A.M.O.; field investigations in the 87 Antarctic cruise of RV "Akademik Mstislav Keldysh" by E.S.C., O.A.Z., P.A.S., S.I.U., and D.G.B. Satellite data analysis by P.A.S. and A.N.S. All authors have read and agreed to the published version of the manuscript.

Funding: This study was conducted within the framework of the Russian state task No. FMWE-2022-0001 (IO RAS) "Assessment of the current state of natural complexes of the Atlantic sector of the Southern Ocean and their multi-period variability (ecosystems, bioproductivity, hydrophysics, hydro- and geochemistry" (A.M.O., O.A.Z.) and CTD data analysis were supported by the Russian Science Foundation grant 22-77-10004 (O.A.Z.), State Assignment KarRC FMEN-2022-0006 (D.G.B.), No. 121090800137-6 "Comprehensive studies of the current state of the ecosystem of the Atlantic sector of Antarctica" (E.Z.S., E.S.C.), Comprehensive environmental studies of the Southern Ocean, No. 0211-2019-0007 (P.A.S), No. 121041400077-1 "Functional, metabolic and toxicological aspects of the existence of hydrobionts and their populations in biotopes with different physico-chemical regime" (N.I.M., V.V.M.) and No. 121122300074-7 "Fundamental research of processes in the climate system that determine the spatial and temporal variability of the natural environment on a global and regional scale" (A.N.S.).

Informed Consent Statement: Not applicable.

Data Availability Statement: Not applicable.

Acknowledgments: The authors are sincerely grateful to the crew of the RV "Akademik Mstislav Keldysh" for their help in the fieldwork. The authors thank the head of the expedition, Morozov E.G., and the deputy head of the expedition, Molodtsova T.N. (IO RAS), for supporting and organizing trawling operations. Special thanks to A.V. Mishin, K.V. Minin, and V.L. Syomin (SIO) for working with trawls and nets that made it possible to obtain krill and salp samples. The authors are also grateful to two anonymous reviewers for valuable comments and suggestions that have significantly improved the quality of the paper.

Conflicts of Interest: The authors declare no conflict of interest.

Ethics Approval: The present research complies with international ethical norms and standards for such scientific research.

References

1. Rintoul, S.R.; Sparrow, M.; Meredith, M.P.; Wadley, V.; Speer, K.; Hofmann, E.; Summerhayes, C.; Urban, E.; Bellerby, R. (Eds.) *The Southern Ocean Observing System: Initial Science and Implementation Strategy*; SCAR: Cambridge, UK, 2012; pp. 1–74.
2. Trathan, P.N.; Hill, S.L. The Importance of Krill Predation in the Southern Ocean. In *Biology and Ecology of Antarctic Krill*; Springer: Cham, Switzerland, 2016; pp. 321–350.
3. Sologub, D.O. Modern Features of Distribution, Biology and Horizontal Migrations of Antarctic Krill (*Euphausia superba*) in the Atlantic Sector of Antarctica. Ph.D. Thesis, VNIRO Publ. House, Moscow, Russia, 2016; pp. 1–247.
4. Nicol, S.; Foster, J. The Fishery for Antarctic Krill: Its Current Status and Management Regime. In *Biology and Ecology of Antarctic Krill*; Springer: Cham, Switzerland, 2016; pp. 387–421.
5. Atkinson, A.; Siegel, V.; Pakhomov, E.A.; Rothery, P.; Loeb, V.; Ross, R.M.; Quetin, L.B.; Schmidt, K.; Fretwell, P.; Murphy, E.J.; et al. Oceanic Circumpolar Habitats of Antarctic Krill. *Mar. Ecol. Prog. Ser.* **2008**, *362*, 1–23. [CrossRef]
6. Siegel, V. Introducing Antarctic Krill Euphausia superba Dana, 1850. In *Biology and Ecology of Antarctic Krill*; Springer: Cham, Switzerland, 2016; pp. 1–20. [CrossRef]
7. Siegel, V.; Watkins, J.L. Distribution, Biomass and Demography of Antarctic Krill, *Euphausia superba*. In *Biology and Ecology of Antarctic Krill*; Springer: Cham, Switzerland, 2016; pp. 21–100.
8. Atkinson, A.; Siegel, V.; Pakhomov, E.; Rothery, P. Long-term Decline in Krill Stock and Increase in Salps within the Southern Ocean. *Nature* **2004**, *432*, 100–103. [CrossRef] [PubMed]
9. Laws, R.M. Ecology of the Southern Ocean. *Amer. Sci.* **1985**, *73*, 26–40.
10. Johnston, N.M.; Murphy, E.J.; Atkinson, A.; Andrew, J.; Constable, A.J.; Cotté, C.; Cox, M.; Daly, K.L.; Driscoll, R.; Flores, H. at al. Status, Change and Futures of Zooplankton in the Southern Ocean. *Front. Ecol. Evol.* **2022**, *9*, 624692. [CrossRef]

11. Samyshev, E.Z. Conclusion on the State of Krill Population and Pelagic Ecosystem in the Western Region of the Atlantic Part of Antarctica in the Pre-winter Period of 1998. *Bull. Ukr. Anarct. Center* **2000**, *3*, 231–236.
12. Samyshev, E.Z. *Antarctic Krill and the Structure of Planktonic Community in its Distribution Area*; USSR Nauka (Acad. of Sci. of the USSR. All-Union Hydrobiol. Soc.): Moscow, Russia; ECOSEA: Sevastopol, Ukraine, 2002; pp. 1–268.
13. Perry, F.A.; Atkinson, A.; Sailley, S.F.; Tarling, G.A.; Hill, S.G.; Lucas, C.H. Habitat Partitioning in Antarctic Krill: Spawning Hotspots and Nursery Areas. *PLoS ONE* **2019**, *14*, eo219325. [CrossRef] [PubMed]
14. Atkinson, A.; Hill, S.L.; Pakhomov, E.; Siegel, V.; Anadon, R.; Chiba, S.; Daly, K.L.; Downie, R.; Fielding, S.; Fretwell, P.; et al. KRILLBASE: A Circumpolar Database of Antarctic Krill and Salp Numerical Densities, 1926–2016. *Earth Syst. Sci. Data.* **2017**, *9*, 193–2107. [CrossRef]
15. Pakhomov, E.A.; Froneman, P.W.; Perissinoto, R. Salp/Krill Interactions in the Southern Ocean: Spatial Segregation and Implications for the Carbon Flux. *Deep Sea Res. II* **2002**, *2*, 1881–1907. [CrossRef]
16. Pakhomov, E.A.; Dubischar, C.; Strass, V.; Brichta, M.; Bathmann, U. The Tunicate *Salpa Thompsoni* Ecology in the Southern Ocean—I. Distribution, Biomass, Demography and Feeding Ecophysiology. *Mar. Biol.* **2006**, *149*, 609–623. [CrossRef]
17. Pakhomov, E.A.; Dubishar, C.; Hunt, B.P.V.; Strass, V.; Cisewski, B.; Siegel, V.; von Harbou, L.; Gurney, L.; Kitchener, J.; Bathmann, U. Biology and Life Cycles of Pelagic Tunicates in the Lazarev Sea, Southern Ocean. *Deep Sea Res. II* **2011**, *58*, 1677–1689. [CrossRef]
18. Lomakin, P.D.; Samyshev, E.Z. Oceanographic Conditions in the Area of the South Shetland Islands in March-April 1997, 1998 and Their Influence on the Distribution of Krill and Salp. *Oceanology* **2004**, *44*, 882–891.
19. Flores, H.; Atkinson, A.; Kawaguchi, S.; Krafft, B.A.; Milinevsky, G.; Nicol, S.; Reiss, C.; Tarling, G.A.; Werner, R.; Rebolledo, E.L.B.; et al. Impact of Climate Change on Antarctic Krill. *Mar. Ecol. Prog. Ser.* **2012**, *458*, 1–19. Available online: https://hal.archives-ouvertes.fr/hal-01250922 (accessed on 21 November 2022). [CrossRef]
20. Pakhomov, E.A.; Hunt, P.V. Trans-Atlantic Variability in Ecology of the Pelagic Tunicate *Salpa thompsoni* near the Antarctic Polar Front. *Deep–Sea Res. II* **2017**, *138*, 126–140. [CrossRef]
21. Groeneveld, Y.; Berger, U.; Henschke, N.; Pakhomov, E.; Reiss, C.; Meyer, B. Blooms of a Key Grazer in the Southern Ocean—An Individual-Based Model of *Salpa thompsoni*. *Prog. Oceanogr.* **2020**, *185*, 102339. [CrossRef]
22. Luo, J.Y.; Stock, C.A.; Henschke, N.; Dunne, J.P.; O'Brien, T.D. Global Ecological and Biogeochemical Impacts of Pelagic Tunicates. *BioRxiv* **2022**, *205*, 102822. [CrossRef]
23. Bombosch, A. Euphausia superba or Salpa thompsoni—Who is Going to Win? 2008. Available online: https://www.coolantarctica.com (accessed on 11 October 2020).
24. Bone, Q.; Carre, C.; Rian, K.P. The Endostyle and Feeding Filter in Salps (Tunicata). *J. Mar. Biol. Ass. UK* **2000**, *80*, 523–534. [CrossRef]
25. Heron, A.C.; Benham, E.E. Individual Growth Rates of Salps in Three Populations. *J. Plankt. Res.* **1984**, *6*, 811–828. [CrossRef]
26. Lüskow, F.; Pakhomov, E.A.; Stukel, M.R.; Décima, M. Biology of *Salpa thompsoni* at the Chatham Rise, New Zeland: Demography, Growth, and Diel Vertical Migration. *Mar. Biol.* **2020**, *167*, 175. [CrossRef]
27. Henschke, N.; Blain, S.; Cherel, Y.; Cotte, C.; Espinasse, B.; Brian, P.V.; Hunt, B.P.V.; Pakhomov, E.A. Population Demographics and Growth Rate of *Salpa Thompsoni* on the Kerguelen Plateau. *J. Mar. Syst.* **2021**, *214*, 103489. [CrossRef]
28. Everett, J.; Baird, M.; Suthers, I. Three-Dimensional Structure of a Swarm of the Salp *Thalia democratica* within a Cold-Core Eddy off Southeast Australia. *J. Geophys. Res.* **2011**, *116*, C12046. [CrossRef]
29. Alcaraz, M.; Almeda, R.; Duarte, C.M.; Horstkotte, B.; Lasternas, S.; Agustí, S. Changes in the C, N, and P Cycles by the Predicted Salps-Krill Shift in the Southern Ocean. *Front. Mar. Scien.* **2014**, *1*, 1–13. [CrossRef]
30. Morozov, E.G.; Flint, M.V.; Orlov, A.M.; Frey, D.I.; Molodtsova, T.N.; Krechik, V.A.; Latushkin, A.A.; Salyuk, P.A.; Murzina, S.A.; Minin, K.V.; et al. Oceanographic and Ecosystem Studies in the Atlantic Sector of Antarctica (Cruise 87 of the Research Vessel Akademik Mstislav Keldysh). *Oceanology* **2022**, *62*, 721–723. [CrossRef]
31. Cross-Calibrated Multi-Platform Ocean Surface Wind. PO. DAAC. Available online: https://www.remss.com (accessed on 20 August 2022).
32. Copernicus Marine Environment Monitoring Service. CMEMS. Available online: https://www.copernicus.eu (accessed on 20 July 2022).
33. Ocean Color WEB. Available online: https://oceancolor.gsfc.nasa.gov/l3/ (accessed on 20 August 2022).
34. Hu, C.; Lee, Z.; Franz, B. Chlorophyll a Algorithms for Oligotrophic Oceans: A Novel Approach Based on Three-Band Reflectance Difference. *J. Geophys. Res.* **2012**, *117*, C01011. [CrossRef]
35. O'Reilly, J.E.; Maritorena, S.; Mitchell, B.G.; Siegel, D.A.; Carder, K.L.; Garver, S.A.; Kahru, M.; McClain, C. Ocean Color Chlorophyll Algorithms for SeaWiFS. *J. Geophys. Res.* **1998**, *103*, 24937–24953. [CrossRef]
36. Visbeck, M. Deep Velocity Profiling Using Lowered Acoustic Doppler Current Profiler: Bottom Track and Inverse Solution. *J. Atmos. Ocean. Tech.* **2002**, *19*, 794–807. [CrossRef]
37. Egbert, G.D.; Erofeeva, S.Y. Efficient Inverse Modeling of Barotropic Ocean Tides. *J. Atmos. Ocean. Tech.* **2002**, *19*, 183–204. [CrossRef]
38. Koblents-Mishke, O.I. Extractive and Non-Extractive Methods for the Determination of Photosynthetic Pigments in Samples. In *Modern Methods for Quantifying the Distribution of Marine Plankton*; Vinogradov, M.E., Ed.; Nauka: Moscow, Russia, 1983; pp. 114–125.

39. Nagornyi, I.G.; Salyuk, P.A.; Maior, A.Y.; Doroshenkov, I.M. A Mobile Complex for On-Line Studying Water Areas and Surface Atmosphere. *Instrum. Exp. Tech.* **2014**, *57*, 68–71. [CrossRef]
40. Bouchard, C.; Mollard, S.; Suzuki, K.; Robert, D.; Fortier, L. Contrasting the Early Life Histories of Sympatric Arctic Gadids Boreogadus Saida and Arctogadus Glacialis in the Canadian Beaufort Sea. *Polar Biol.* **2016**, *39*, 1005–1022. [CrossRef]
41. Kobyliansky, S.G.; Orlov, A.M.; Gordeeva, N.V. Composition of Deepsea Pelagic Ichthyocenes of the Southern Atlantic, from Waters of the Range of the Mid-Atlantic and Walvis Ridges. *J. Ichthyol.* **2010**, *50*, 932–50949. [CrossRef]
42. Bongo Plankton Net. Available online: https://www.nhbs.com/bongo-plankton-net (accessed on 20 August 2022).
43. Siegel, V.; Kawaguchi, S.; Ward, P.; Litvinov, F.; Sushin, V.; Loeb, V.; Watkins, J. Krill Demography and Large-Scale Distribution in the Southwest Atlantic During January/February 2000. *Deep Sea Res. II* **2004**, *51*, 1253–1273. [CrossRef]
44. Morris, D.J.; Watkins, J.L.; Ricketts, C.; Buchholz, F.; Priddle, J. An Assessment of the Merits of Length and Weight Measurements of Antarctic Krill *Euphausia superba*. *Brit. Ant. Surv. Bull.* **1988**, *79*, 27–50.
45. Anonymous. *Scientific Observers Manual*; CCAMLR: Hobart, Australia, 2011; pp. 1–232.
46. Petrov, A.F.; Shust, K.V.; Piyanova, S.; Uryupova, E.; Gordeev, I.I.; Sitov, A.M.; Demina, S.N. *Guidelines for the Collection and Processing of Fishing and Biological Data on Aquatic Bioresources of Antarctica for the Russian Scientific Observers in the CCAMLR Convention Area*; VNIRO Publ. House: Moscow, Russia, 2014; pp. 45–53.
47. Makarov, R.R.; Denys, C.J. Stages of Sexual Maturity of *Euphausia superba* Dana. *BIOMASS Handbook* **1980**, *11*, 1–11.
48. Meyer, B.; Auerswald, L.; Siegel, V.; Spahic, S.; Pape, C.; Fach, B.A.; Teschke, M.; Lopata, A.L.; Fuentes, V. Seasonal Variation in Body Composition, Metabolic Activity, Feeding and Growth of Adult Krill *Euphausia superba* in the Lazarev Sea. *Mar. Ecol. Prog. Ser.* **2010**, *398*, 1–18. [CrossRef]
49. Watkins, J.L.; Morris, D.J.; Ricketts, C. Nocturnal Changes in the Mean Length of a Euphausiid Population: Vertical Migration, Net Avoidance or Experimental Error? *Mar. Biol.* **1985**, *86*, 123–127. [CrossRef]
50. Tokarczyk, R. Classification of Water Masses in the Bransfield Strait and Southern Part of the Drake Passage Using a Method of Statistical Multidimensional Analysis. *Polish Polar Res.* **1987**, *8*, 333–336.
51. Orsi, A.H.; Nowlin, W.D.; Whitworth III, T. On the Circulation and Stratification of the Weddell Gyre. *Deep-Sea Res. I* **1993**, *40*, 169–203. [CrossRef]
52. Heywood, K.J.; Garabato, A.C.N.; Stevens, D.P.; Muench, R.D. On the Fate of the Antarctic Slope Front and the Origin of the Weddell Front. *J. Geophys. Res.* **2004**, *109*, C06021. [CrossRef]
53. Dorschel, B.; Gutt, J.; Huhn, O.; Bracher, A.; Huntemann, M.; Huneke, W.; Gebhardt, C.; Schroder, M.; Herr, H. Environmental Information for a Marine Ecosystem Research Approach for the Northern Antarctic Peninsula (RV Polarstern expedition PS81, ANT-XXIX/3). *Polar Biol.* **2016**, *39*, 765–787. [CrossRef]
54. Krechik, V.A.; Frey, D.I.; Morozov, E.G. Peculiarities of Water Circulation in the Central Part of the Bransfield Strait in January 2020. *Dokl. Earth Sci.* **2021**, *496*, 92–95. [CrossRef]
55. Morozov, E.G.; Flint, M.V.; Spiridonov, V.A. *Antarctic Peninsula Region of the Southern Ocean*; Springer: Cham, Switzerland, 2021; pp. 1–455. [CrossRef]
56. Huneke, W.G.; Huhn, O.; Schroeder, M. Water Masses in the Bransfield Strait and Adjacent Seas, Austral Summer 2013. *Polar Biol.* **2016**, *39*, 789–798. [CrossRef]
57. Krek, A.V.; Krek, E.V.; Krechik, V.A. The Circulation and Mixing Zone in the Antarctic Sound in February 2020. In *Antarctic Peninsula Region of the Southern Ocean*; Springer: Cham, Switzerland, 2021; pp. 83–99. [CrossRef]
58. van Caspel, M.; Hellmer, H.H.; Mata, M.M. On the Ventilation of Bransfield Strait Deep Basins. *Deep-Sea Res. II* **2017**, *149*, 25–30. [CrossRef]
59. Kang, S.H.; Kang, J.S.; Lee, S.; Chung, K.H.; Kim, D.; Park, M.G. Antarctic Phytoplankton Assemblages in the Marginal Ice Zone of the Northwestern Weddell Sea. *J. Plankt. Res.* **2001**, *23*, 333–352. [CrossRef]
60. Nunes, S.; Latasa, M.; Delgado, M.; Emelianov, M.; Simó, R.; Estrada, M. Phytoplankton Community Structure in Contrasting Ecosystems of the Southern Ocean: South Georgia, South Orkneys and Western Antarctic Peninsula. *Deep-Sea Res. I* **2019**, *151*, 103059. [CrossRef]
61. Mendes, C.R.B.; de Souza, M.S.; Garcia, V.M.T.; Leal, M.C.; Brotas, V.; Garcia, C.A.E. Dynamics of Phytoplankton Communities During Late Summer Around the Tip of the Antarctic Peninsula. *Deep-Sea Res. I.* **2012**, *65*, 1–14. [CrossRef]
62. Ferreira, A.; Brito, A.C.; Mendes, C.R.; Brotas, V.; Costa, R.R.; Guerreiro, C.V.; Sá, C.; Jackson, T. OC4-SO: A New Chlorophyll-a Algorithm for the Western Antarctic Peninsula Using Multi-Sensor Satellite Data. *Remote Sens.* **2022**, *14*, 1052. [CrossRef]
63. Pereira, E.S.; Garcia, C.A.E. Evaluation of Satellite-Derived MODIS Chlorophyll Algorithms in the Northern Antarctic Peninsula. *Deep-Sea Res. II* **2018**, *149*, 124–137. [CrossRef]
64. Meredith, M.P.; Renfrew, I.A.; Clarke, A.; King, J.C.; Brandon, M.A. Impact of the 1997/98 ENSO on the Upper Waters of Marguerite Bay, Western Antarctic Peninsula *J. Geophys. Res.* **2004**, *109*, C09013. [CrossRef]
65. Atkinson, A.; Shreeve, R.; Hirst, A.; Rothery, P.; Tarling, G.; Pond, D.; Korb, R.; Murphy, E.; Watkins, J.L. Natural Growth Rates in Antarctic Krill (*Euphausia Superba*): II. Predictive Models Based on Food, Temperature, Body Length, Sex, and Maturity Stage. *Limnol. Oceanogr.* **2006**, *51*, 973–987. [CrossRef]
66. Tarling, G.A.; Cuzin-Roudy, J.; Thorpe, S.E.; Shreeve, R.S.; Ward, P.; Murphy, E.J. Recruitment of Antarctic Krill *Euphausia Superba* in the South Georgia Region: Adult Fecundity and the Fate of Larvae. *Mar. Ecol. Prog. Ser.* **2007**, *331*, 161–179. [CrossRef]

67. Wiedenmann, J.; Cresswell, K.; Mangel, M. Temperature-Dependent Growth of Antarctic Krill: Predictions for a Changing Climate from a Cohort Model. *Mar. Ecol. Prog. Ser.* **2008**, *358*, 191–202. [CrossRef]
68. Spiridonov, V.A.; Zalota, A.K.; Yakovenko, V.A.; Gorbatenko, K.M. Population Composition and Transport of Antarctic Krill Juveniles in the Powell Basin (Northwestern Part of the Weddell Sea) in January 2020. *Tr. VNIRO* **2020**, *181*, 33–51. [CrossRef]
69. Yakovenko, V.A.; Spiridonov, V.A.; Gorbatenko, K.M.; Shadrin, N.V.; Samyshev, E.Z.; Minkina, N.I. Macro- and Mesozooplankton in the Powell Basin (Antarctica): Species Composition and Distribution of Abundance and Biomass in February 2020. In *Antarctic Peninsula Region of the Southern Ocean*; Springer: Cham, Switzerland, 2021; pp. 131–141. [CrossRef]
70. Hereu, C.M.; Suárez-Morales, E.; Lavaniegos, B.E. Record of the Rare Oceanic Salp *Helicosalpa Komaii* (Tunicata: Thaliacea: Salpida) in the Northeast Pacific. *Rev. Mex. Biodiver.* **2014**, *85*, 624–629. [CrossRef]
71. Kasatkina, S.M.; Abramov, A.M.; Sokolov, M.Y. Biomass and Distribution of Antarctic Krill in the Antarctic Atlantic Area in January-February 2020. *Tr. AtlantNIRO* **2021**, *5*, 49–61.
72. Sytov, A.M.; Kozlov, D.A. Dimensional Composition and Biological Characteristics of Antarctic Krill Euphausia Superba in the Antarctic Part of the Atlantic in January-March 2020. *Tr. AtlantNIRO* **2021**, *5*, 101–115.
73. Krag, L.A.; Herrmann, B.; Iversen, S.A.; Engas, A.; Nordrum, S.; Krafft, B.A. Size Selection of Antarctic Krill (*Euphausia superba*) in Trawls. *PLoS ONE* **2014**, *9*, e102168. [CrossRef]
74. Wang, Z.; Tang, H.; Herrmann, B.; Xu, L. Catch Pattern for Antarctic Krill (*Euphausia superba*) of Different Commercial Trawls in Similar Times and Overlapping Fishing Grounds. Grounds. *Front. Mar. Sci.* **2021**, *8*, 670663. [CrossRef]
75. Cox, M.J.; Borchers, D.L.; Demer, D.A.; Cutter, G.R.; Brierley, A.S. Estimating the Density of Antarctic Krill (*Euphausia Superba)* from Multibeam Echo-Sounder Observations Using Distance Sampling Methods. *J. R. Stat. Soc. Ser. C App. Statist.* **2011**, *60*, 301–316. [CrossRef]
76. Kasatkina, S.M. Methodical Aspects of Acoustic Survey for Antarctic Krill in the CCAMLR Convention are. *Tr. AtlantNIRO* **2021**, *5*, 39–48, ISSN: 2541-9692.
77. Bargmann, H.E. The Development and Life History of Adolescent and Adult Krill *Euphausia superba*. *Discovery Rep.* **1945**, *XXIII*, 103–178.
78. Fraser, F.G. On the Development and Distribution of the Young Stages of Krill (*Euphausia superba*). *Discovery Rep.* **1936**, *XIV*, 1–192. [CrossRef]
79. Marr, J.W.S. The Natural History and Geography of the Antarctic Krill (*Euphausia superba* Dana). *Discovery Rep.* **1962**, *XXXII*, 33–464.
80. Shvetsov, V.V.; Makarov, R.R. On the Biology of Antarctic Krill. *Tr. VNIRO.* **1969**, *LXVI*, 177–206.
81. Barkley, E. Nahrung und Filterapparat des Walkrebschens *Euphausia superba* Dana. *Z. Fisch. Deren Hilfswiss.* **1940**, *1*, 65–156.
82. Brotz, L.; Cheung, W.W.L.; Kleisner, K.; Pakhomov, E.; Pauly, D. Increasing Jellyfish Populations: Trends in Large Marine Ecosystems. *Hydrobiol.* **2012**, *690*, 3–20. [CrossRef]
83. Constable, A.J.; Melbourne-Thomas, J.; Corney, S.P.; Arrigo, K.R.; Barbraud, C.; Barnes, D.K.A.; Bindoff, N.L.; Boyd, P.W.; Brandt, A.; Costa, D.P. at al. Climate Change and Southern Ocean Ecosystems I: How Changes in Physical Habitats Directly Affect Marine Biota. *Glob. Change Biol.* **2014**, *20*, 3004–3025. [CrossRef] [PubMed]
84. Henschke, N.; Everett, J.D.; Richardson, A.J.; Suthers, I.M. Rethinking the Role of Salps in the Ocean. *Trends Ecol. Evol.* **2016**, *31*, 720–733. [CrossRef]
85. Shnar, V.N.; Kasatkina, S.M. Long-Term Variability of Environmental Conditions and Distribution of Antarctic Krill *Euphausia Superba* in the Sub-Region of the Antarctic Peninsula in 1970-2020. *Tr. AtlantNIRO* **2021**, *5*, 101–110.
86. Atkinson, A.; Hill, S.L.; Pakhomov, E.A.; Siegel, V.; Reiss, C.S.; Loeb, V.J.; Steinberg, D.K.; Schmidt, K.; Tarling, G.A.; Gerrish, L.; et al. Krill (*Euphausia superba*) Distribution Contracts Southward During Rapid Regional Warming. *Nat. Clim. Chang.* **2019**, *9*, 142–147. [CrossRef]
87. Loeb, V.; Siegel, V.; Holm-Hansen, O.; Hewitt, R.; Fraser, W.; Trivelpiece, W.; Trivelpiece, S. Effects of Sea-Ice Extent and Krill or Salp Dominance on the Antarctic Food Web. *Nature* **1997**, *387*, 897–900. [CrossRef]
88. Ross, R.; Quetin, L.; Newberger, T.; Shaw, T.; Jones, J.; Oakes, S.; Moore, K. Trends, Cycles, Interannual Variability for Three Pelagic Species West of the Antarctic Peninsula 1993–2008. *Mar. Ecol. Prog. Ser.* **2014**, *515*, 11–32. [CrossRef]
89. Minkina, N.I.; Samyshev, E.Z.; Pakhomov, E.A.; Melnikov, V.V. Temporal and Satial Variability of Energy Exchange in Antarctic Salps. *Res. Square* **2022**. [CrossRef]
90. Atkinson, A.; Siegel, V.; Pakhomov, E.A.; Jessopp, M.J.; Loeb, V. A Re-Appraisal of the Total Biomass and Annual Production of Antarctic Krill. *Deep-Sea Res. I* **2009**, *56*, 727–740. [CrossRef]
91. Murphy, E.J.; Watkins, J.L.; Trathan, P.; Reid, K.; Meredith, M.P.; Thorpe, S.E.; Fleming, A.H. Spatial and Temporal Operation of the Scotia Sea Ecosystem: A Review of Large-Scale Links in a Krill Centred Food Web. *Philosophical Trans. R. Soc. B. Biol. Sci.* **2007**, *362*, 113–148. [CrossRef] [PubMed]
92. Loeb, V.J.; Santora, J.A. Population Dynamics of *Salpa Thompsoni* Near the Antarctic Peninsula: Growth Rates and Interannual Variations in Reproductive Activity (1993–2009). *Prog. Oceanogr.* **2012**, *96*, 93–107. [CrossRef]
93. Kasyan, V.V.; Bitiutskii, D.G.; Voronin, V.P.; Zuev, O.A.; Kalinina, O.Y.; Kolbasova, G.D.; Mishin, A.V.; Murzina, S.A.; Kolbasova, G.D.; Voronin, V.P.; et al. Composition and Distribution of Plankton Communities in the Atlantic Sector of the Southern Ocean. *Diversity* **2022**, *14*, 923. [CrossRef]